PHYSICAL REVIEW D **90,** 103010 (2014)

Impact of polarization on the intrinsic cosmic microwave background bispectrum

Guido W. Pettinari,[1,2,*] Christian Fidler,[2] Robert Crittenden,[2] Kazuya Koyama,[2] Antony Lewis,[1] and David Wands[2]

[1]*Department of Physics and Astronomy, University of Sussex, Brighton BN1 9QH, United Kingdom*

[2]*Institute of Cosmology and Gravitation, University of Portsmouth, Portsmouth PO1 3FX, United Kingdom*

(Received 12 June 2014; published 24 November 2014)

We compute the cosmic microwave background (CMB) bispectrum induced by the evolution of the primordial density perturbations, including for the first time both temperature and polarization using a second-order Boltzmann code. We show that including polarization can increase the signal-to-noise by a factor 4 with respect to temperature alone. We find the expected signal-to-noise for this intrinsic bispectrum of $S/N = 3.8, 2.9, 1.6$ and 0.5 for an ideal experiment with an angular resolution of $\ell_{\rm max} = 3000$, the proposed CMB surveys PRISM and COrE, and Planck's polarized data, respectively; the bulk of this signal comes from E-mode polarization and from squeezed configurations. We discuss how CMB lensing is expected to reduce these estimates as it suppresses the bispectrum for squeezed configurations and contributes to the noise in the estimator. We find that the presence of the intrinsic bispectrum will bias a measurement of primordial non-Gaussianity of local type by $f_{\rm NL}^{\rm intr} = 0.66$ for an ideal experiment with $\ell_{\rm max} = 3000$. Finally, we verify the robustness of our results by recovering the analytic approximation for the squeezed-limit bispectrum in the general polarized case.

DOI: 10.1103/PhysRevD.90.103010 PACS numbers: 98.70.Vc, 98.62.Sb, 98.80.Es

I. INTRODUCTION

The three-point function, or bispectrum, of the cosmic microwave background (CMB) is directly linked to non-Gaussian features in the primordial fluctuations from which the CMB evolved [1–5]. Measuring the CMB bispectrum is therefore equivalent to opening a window to the early Universe. In particular the temperature maps measured by the Planck CMB survey [6] provide the most stringent constraint on the amplitude $f_{\rm NL}$ of primordial non-Gaussianity of the local type [1,7,8]: $f_{\rm NL} = 2.7 \pm 5.8$. Furthermore, the polarized maps, expected from Planck by the end of 2014, will be used to refine the $f_{\rm NL}$ measurement and reduce the uncertainty by approximately a factor 2 [4,9–12].

However not all of the observed non-Gaussianity is of primordial origin. Indeed, a bispectrum arises in the CMB even for Gaussian initial conditions in the primordial curvature perturbation [13] due to nonlinear dynamics such as CMB photons scattering off free electrons and their propagation along a perturbed geodesic in an inhomogeneous Universe. This *intrinsic bispectrum* is an interesting signal in its own right as it contains information on such processes. Furthermore, if not correctly estimated and subtracted from the CMB maps, it will provide a bias in the estimate of primordial $f_{\rm NL}$.

Computing the intrinsic bispectrum requires solving the Einstein and Boltzmann equations up to second order in the cosmological perturbations. These have been studied in great detail [14–19] and, even though approximate solutions have been found in specific limits [20–29], they require a numerical treatment. Numerical convergence is now being reached as the latest codes [30–33] obtain consistent results. For temperature alone, these codes find the bias induced on $f_{\rm NL}$ to be of order unity, and the intrinsic bispectrum to be unobservable by Planck, its signal-to-noise ratio reaching unity only for an ideal experiment with an angular resolution of $\ell_{\rm max} = 3000$.

In this paper, we extend the studies discussed above by including for the first time CMB polarization and show that the intrinsic bispectrum signal is enhanced considerably compared to the primordial signals, making it potentially observable in the next generation CMB missions, such as COrE [34] and PRISM [35]. We also explore the impact that gravitational lensing has on the observability of the intrinsic bispectrum, both by reducing the amplitude of the intrinsic signal and by providing an additional source of noise in the measurement of the bispectra.

II. METHOD

The dynamics of CMB photons is governed by the Boltzmann equation, which consists of a Liouville term accounting for photon propagation in an inhomogeneous space-time and a collision term describing photon interactions, i.e., Compton scattering off free electrons. We characterize photons by their brightness moments Δ_n. The composite index n includes the angular harmonic indices ℓm and the field index X, denoting either intensity ($X = T$)

*g.pettinari@sussex.ac.uk

or linear polarization ($X = E, B$). The Boltzmann equation to second order for Δ_n reads

$$\dot{\Delta}_n + k\Sigma_{nn'}\Delta_{n'} + \mathcal{M}_n + \mathcal{Q}_n^L = C_n, \tag{1}$$

where k is the Fourier wave vector of the perturbation, and the free-streaming matrix $\Sigma_{nn'}$ encodes the excitation of high-ℓ moments over time. We have denoted the terms containing only gravitational perturbations by $\mathcal{M}_n$, while $\mathcal{Q}_n^L$ describes the effect of gravity on the photon perturbations, that is, the redshift, time-delay and lensing effects. The collision term

$$C_n = -|\dot{\kappa}|(\Delta_n - \Gamma_{nn'}\Delta_{n'} - \mathcal{Q}_n^C) \tag{2}$$

is proportional to the Compton scattering rate $|\dot{\kappa}|$ and consists of the purely second-order gain and loss terms and quadratic contributions $|\dot{\kappa}|\mathcal{Q}_n^C$. A detailed description of all terms can be found in Refs. [32,36,37].

After recombination photons stream freely, so that at conformal time η the higher multipoles with $\ell \approx k(\eta - \eta_{\rm rec})$ are excited, making the numerical computation of the photon moments up to today (η_0) impractical using Eq. (1). In SONG we instead use the line-of-sight integration [38]:

$$\Delta_n(\eta_0) = \int_0^{\eta_0} d\eta e^{-\kappa(\eta)} j_{nn'}(k(\eta_0 - \eta))\mathcal{S}_{n'}(\eta), \tag{3}$$

with the streaming functions $j_{nn'}$ specified in Refs. [37,39], and the line-of-sight source function $\mathcal{S}_n$ given by

$$\mathcal{S}_n = -\mathcal{M}_n - \mathcal{Q}_n^L + |\dot{\kappa}|(\Gamma_{nn'}\Delta_{n'} + \mathcal{Q}_n^C). \tag{4}$$

We first solve the full second-order Boltzmann-Einstein hierarchy to build $\mathcal{S}_n$ until the time of recombination and then compute the line-of-sight integral in Eq. (3) to obtain Δ_n today.

It was recently shown [33,40] that the lensing and time-delay terms in Eq. (4) correspond to the well-known CMB-lensing bispectrum in the remapping approach [41] plus a small residual. We therefore do not consider these terms in $\mathcal{S}_n$. We do include the redshift term by using the $\tilde{\Delta}$ transformation of variables first introduced in Ref. [30] and later generalized to the polarized case in Ref. [36].

After using the line-of-sight integration to obtain $\Delta_n(\eta_0)$, we relate it to the bolometric temperature perturbation $a^X_{\ell m}$ [36,42,43] and compute its full-sky bispectrum:

$$B^{XYZ}_{\ell_1\ell_2\ell_3} = \sum_{m_1 m_2 m_3} \begin{pmatrix} \ell_1 & \ell_2 & \ell_3 \\ m_1 & m_2 & m_3 \end{pmatrix} \langle a^X_{\ell_1 m_1} a^Y_{\ell_2 m_2} a^Z_{\ell_3 m_3}\rangle$$
$$= \begin{pmatrix} \ell_1 & \ell_2 & \ell_3 \\ 0 & 0 & 0 \end{pmatrix} b^{XYZ}_{\ell_1\ell_2\ell_3}, \tag{5}$$

where X, Y, Z are either T or E. In Ref. [32] we focused on the unpolarized scalar contributions to the bispectrum, corresponding to the $m = 0$ sources in Eq. (4). In this paper, we also include $m \neq 0$ contributions up to $|m| = 3$ following Ref. [37] and find that they are subdominant with respect to the $m = 0$ modes as they consist of about 3% of the total signal.

In the calculations below, we have assumed the Planck best-fit ΛCDM cosmology [44] where $h = 0.678$, $\Omega_b = 0.0483$, $\Omega_{\rm cdm} = 0.259$, $\Omega_\Lambda = 0.693$, $A_s = 2.214 \times 10^{-9}$, $n_s = 0.961$, $N_{\rm eff} = 3.04$, and $\kappa_{\rm reio} = 0.095$. We also assume adiabatic initial conditions with a vanishing primordial tensor-to-scalar ratio ($r = 0$) and non-Gaussianity ($f_{\rm NL} = 0$).

III. POLARIZATION IMPACT

For squeezed configurations ($\ell_1 \ll \ell_2, \ell_3$), where the long-wavelength mode is within the horizon today but was not at recombination ($\ell_1 \ll 200$), the intrinsic bispectrum is known analytically. In this case, the superhorizon curvature perturbation at recombination, ζ, acts as a perturbation to the background curvature that dilates the observed angular scale of the small-scale CMB anisotropies. Large and small scales are thus correlated and a squeezed intrinsic bispectrum arises that is proportional to the correlation between the large-scale CMB anisotropies and ζ. In multipole space, a dilation corresponds to a sideways shift in ℓ, so that the more sharply peaked the small-scale power spectrum, the bigger the change in power. As a result, the intrinsic bispectrum in the squeezed limit is proportional to the derivative of the small-scale power spectrum [26–29]:

$$b^{{\rm sq},XYZ}_{\ell_1\ell_2\ell_3} = -\frac{1}{2} C^{X\zeta}_{\ell_1}\left[\frac{{\rm d}(\ell_2{}^2 C^{YZ}_{\ell_2})}{\ell_2 {\rm d}\ell_2} + \frac{{\rm d}(\ell_3{}^2 C^{YZ}_{\ell_3})}{\ell_3 {\rm d}\ell_3}\right]$$
$$+ C^{XT}_{\ell_1}[\delta_{ZT} C^{YT}_{\ell_2} + \delta_{YT} C^{ZT}_{\ell_3}], \tag{6}$$

where the angular power spectra are defined by $\langle a^X_{\ell m} a^{Y*}_{\ell' m'}\rangle \equiv C^{XY}_\ell \delta_{\ell\ell'}\delta_{mm'}$. The second line in Eq. (6) represents the subdominant effect known as redshift modulation [29]. In Fig. 1, we show that SONG's numerical bispectra match the analytical approximation in the squeezed limit at percent-level precision.

In SONG we truncate the line-of-sight integration in Eq. (3) at recombination and thus neglect the second-order scattering sources at reionization. Their computation is challenging as it involves summations over high-ℓ multipoles at late times. In any case, a second-order treatment would still be insufficient, as nonlinear effects are relevant at the time of reionization. We do however include reionization at the background and linear level. The squeezed formula of Eq. (6) works at the same level, hence the match with SONG for squeezed shapes.

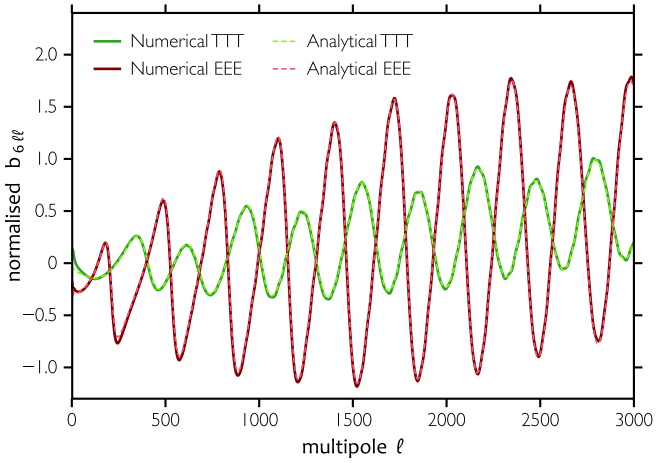

FIG. 1 (color online). Numerical intrinsic bispectrum produced by SONG together with the squeezed-limit approximation in Eq. (6), with $\ell_1 = 6$ and $\ell_2 = \ell_3 = \ell$. We normalize the curves to the squeezed limit for the local-type bispectrum [1,7] with $f_{\rm NL} = 5$, that is, $6C_{\ell_1}^{X\zeta}(C_{\ell_2}^{YZ} + C_{\ell_3}^{YZ})$.

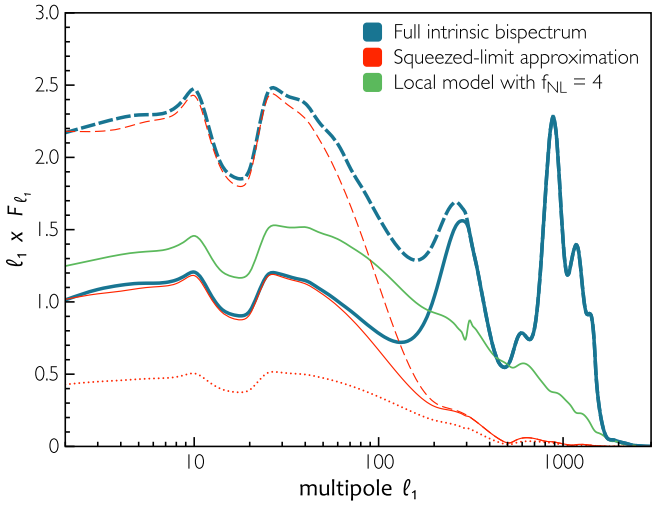

FIG. 2 (color online). Inverse variance of the intrinsic bispectrum as a function of its smallest multipole ℓ_1, considering an ideal experiment with $\ell_{\rm max} = 3000$. The area below each curve is proportional to $(S/N)^2$. The full bispectrum computed with SONG (thick blue lines) exhibits distinctive peaks on subhorizon scales ($\ell_1 > 100$), while on larger scales it tracks the squeezed-limit approximation (thin red lines). The dashed lines do not include lensing variance, which reduces the signal-to-noise only on superhorizon scales; the lensed bispectrum in the squeezed limit is shown by the dotted line. For reference, we include the curve expected from a local-type bispectrum with $f_{\rm NL} = 4$ (solid green line).

The linear temperature anisotropies observed today are sourced by density and velocity perturbations at recombination. Since these are out of phase in ℓ space, the resulting acoustic peaks are blurred. On the other hand, the peaks of the E polarization spectrum are sharper as their only source is the quadrupole induced by Compton scattering. It follows that the logarithmic derivatives in Eq. (6) normalized to C_ℓ^{YZ} will be larger for polarization than for temperature. This enhancement is about a factor 2.5 in magnitude across the whole ℓ range (Fig. 1) and leads to a larger signal-to-noise ratio for the polarized bispectra.

The observability of the intrinsic bispectrum is quantified by its signal-to-noise ratio $S/N = \sqrt{F^{\rm intr,intr}}$, while the bias it induces on a measurement of local-type $f_{\rm NL}$ is $f_{\rm NL}^{\rm intr} = F^{\rm loc,intr}/F^{\rm loc,loc}$, with $F^{(i),(j)}$ the Fisher matrix element in the general polarized case [1,9,12,41]:

$$F^{(i),(j)} = \sum_{ABC,XYZ} \sum_{2\le\ell_1\le\ell_2\le\ell_3}^{\ell_{\rm max}} \frac{1}{\Delta_{\ell_1\ell_2\ell_3}} \times B^{(i),ABC}_{\ell_1\ell_2\ell_3} (\tilde{C}^{-1}_{\rm tot})^{AX}_{\ell_1} (\tilde{C}^{-1}_{\rm tot})^{BY}_{\ell_2} (\tilde{C}^{-1}_{\rm tot})^{CZ}_{\ell_3} B^{(j),XYZ}_{\ell_1\ell_2\ell_3}, \quad (7)$$

where $\Delta_{\ell_1\ell_2\ell_3} = 1, 2, 6$ for triangles with no, two or three equal sides, $\ell_{\rm max}$ is limited by the finite angular resolution of the survey and $\tilde{C}_{\rm tot}^{XY}$ is given by the sum of the lensed spectrum and a noise term to account for the sensitivity of the survey [45,46]. The first sum involves all possible pairs of the eight T and E bispectra, while the product of three $\tilde{C}_{\rm tot}^{-1}$ represents their covariance.

In Fig. 2 we show $F^{\rm intr,intr}$ as a function of ℓ_1, the smallest multipole in the sum, for an ideal CMB survey with a resolution of $\ell_{\rm max} = 3000$. On superhorizon scales ($\ell_1 \ll 200$), the intrinsic bispectrum computed by SONG agrees well with the squeezed-limit formula, as expected. The subhorizon effects computed by SONG become important for $\ell_1 > 100$ and give rise to several acoustic peaks. The signal associated to the subhorizon peaks is given by the square root of the area below the curve and amounts to $S/N = 1.6$ and 2.7 for $\ell_{\rm max} = 3000$ and 4000, respectively; most of this signal comes from squeezed triangles. Note that these effects cannot be treated in the analytical approximation in Eq. (6) and hence need to be computed using a full second-order code like SONG. Furthermore, we find that the relative importance of the subhorizon effects increases with $\ell_{\rm max}$.

IV. LENSING EFFECTS

The Fisher matrix estimator of Eq. (7) is optimal only under the assumption of a nearly Gaussian CMB. However, the gravitational lensing of CMB photons generates a non-Gaussian signal that must be accounted for in the covariance matrix; not doing so would overestimate the significance for a detection of the intrinsic bispectrum [41,47]. We account for this *lensing variance* in the estimator following the analytic approach of Ref. [41], which is valid for squeezed configurations.

We find that lensing variance degrades the intrinsic signal from $\ell_1 < 200$ by approximately a factor $\sqrt{2}$, while leaving the signal from smaller scales unaltered, as can be seen by comparing the dashed and solid curves in Fig. 2.

The reason is that most of the signal below $\ell_1 < 200$ comes the squeezed configurations described by the analytical formula in Eq. (6), which are highly degenerate with the isotropic part of lensing (i.e., convergence) [26,27,29]. As a result, the added noise from lensing convergence significantly reduces our ability to detect the intrinsic bispectrum for $\ell_1 < 200$. On the other hand, we find that the intrinsic signal does not correlate significantly with convergence or shear modes on smaller scales and is thus not affected by lensing variance. After correcting for lensing variance, the subhorizon effects constitute about 40% and 50% of the intrinsic signal squared for $\ell_{\rm max} = 3000$ and 4000, respectively, and a larger fraction for higher resolutions.

Two other effects of gravitational lensing may affect the measurement of the intrinsic bispectrum. First, the correlation between the photon intensity and the lensing deflection angle results in the emergence of a CMB-lensing bispectrum [48–50] which was recently detected by the Planck experiment [6] and corresponds to the lensing terms we dropped in the line-of-sight integration. The isotropic part of the CMB-lensing bispectrum is known to be degenerate with the intrinsic bispectrum [26,27,29] in the squeezed limit and might therefore contaminate a measurement of the latter. However, we find that the intrinsic and lensing bispectra have a correlation of 0.6% and, by marginalizing over the latter bispectrum, that the intrinsic S/N is degraded only by about 0.002%. These numbers suggest that the CMB-lensing bispectrum is different enough from the intrinsic bispectrum to allow a clear separation of the effects, in analogy to the case of the local $f_{\rm NL}$ template [6,41]. Note that this separation cannot be used to reduce the impact of lensing variance, as the signal cannot be used to reduce the noise in the estimator.

Secondly, CMB lensing distorts the observed shape of the intrinsic bispectrum in a nonperturbative way. In the squeezed limit, the lensed bispectrum is obtained by substituting the power spectrum C_ℓ^{YZ} in Eq. (6) with its lensed counterpart $\tilde{C}_\ell^{YZ}$ [29,41]. This results in a smaller bispectrum as the derivatives in Eq. (6) now act on a smoother function. The S/N from squeezed configurations is consequently reduced by a factor of approximately $\sqrt{2}$ for $\ell_{\rm max} = 3000$, as can be seen by comparing the solid and dotted red curves in Fig. 2. However, this suppression is only valid in the squeezed case; for arbitrary configurations one has to resort to a more general approach [47,51,52], which we will address in future work.

V. OBSERVATIONAL IMPLICATIONS

In Fig. 3 we present the signal-to-noise ratio of the intrinsic bispectrum as a function of the maximum resolution $\ell_{\rm max}$ for four experiments: an ideal experiment, the proposed CMB surveys PRISM [35] and COrE [34], and Planck polarization data. The angular resolution of the CMB survey strongly affects the detectability of the intrinsic bispectrum. With a resolution of $\ell_{\rm max} = 3000$, an ideal experiment would observe the intrinsic bispectrum at the 2.7σ level, while PRISM, COrE and Planck polarized data would yield 2.1σ, 1.3σ, and 0.46σ, respectively. When we account for the lensing of the bispectrum in the squeezed regime via the analytical formula in Eq. (6), these numbers reduce to 2.1σ, 1.8σ, 1.1σ, and 0.41σ.

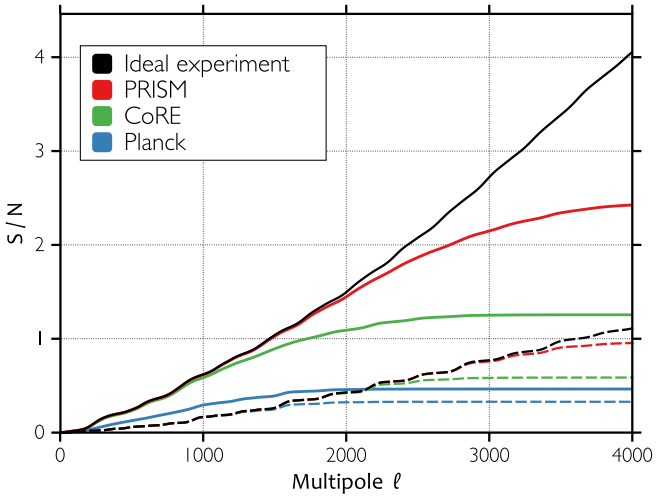

FIG. 3 (color online). Signal-to-noise ratio of the intrinsic bispectrum for the four experiments described in the text as a function of the maximum resolution $\ell_{\rm max}$, including lensing variance and excluding the lensing of the bispectrum. The solid curves include all eight bispectra, the dashed ones only temperature.

Figure 3 also shows that most of the signal in the intrinsic bispectrum comes from E polarization rather than temperature. The reason is twofold. First, the dilation effect that generates the intrinsic bispectrum on squeezed scales is ~2.5 times more efficient for polarization than for temperature, as shown in Fig. 1. Secondly, as long as the instrumental noise is low enough, both temperature and polarization are sample-variance limited, so that the polarization bispectrum variance is also suppressed compared to that of the temperature. In principle, the same argument applies to B polarization. The intrinsic B signal, however, is sourced by nonscalar sources that are geometrically suppressed [36], making it smaller than the E signal and thus likely to be dominated by lensing [53,54] and instrumental noise.

We find the bias to the local-type $f_{\rm NL}$ for an ideal experiment with resolution $\ell_{\rm max} = 3000$ to be $f_{\rm NL}^{\rm intr} = 1.33$, 1.50, and 1.51 for temperature, polarization and the two probes combined, respectively. Including lensing variance reduces the bias to $f_{\rm NL}^{\rm intr} = 0.95, 0.61, 0.66$. This suppression is due to the intrinsic bispectrum being affected by lensing variance more than the local template. The bias is further reduced by varying the experimental setup: for PRISM, COrE and Planck polarized data we find $f_{\rm NL}^{\rm intr} = 0.58, 0.45, 0.37$, respectively, considering lensing variance and both temperature and polarization.

VI. CONCLUSIONS

Including polarization is crucial to extract all the information contained in the CMB. In this paper we have extended previous analyses of the intrinsic bispectrum [31–33] and shown that it is particularly sensitive to polarization due to the sharp acoustic peaks in the E-mode power spectrum. Using a Fisher matrix approach, we showed that the eight combined bispectra generate a signal-to-noise ratio 4 times larger with respect to the temperature-only case, making the signal potentially observable at the 2σ level in future high-resolution missions, such as PRISM [35] or an improved version of COrE [34]. Despite the enhancement of the intrinsic signal, we still find its contamination to the local-type primordial $f_{\rm NL}$ to be comparable to the unpolarized case.

For squeezed configurations, the gravitational lensing of CMB photons limits the possibility of observing the intrinsic bispectrum by adding extra variance and by reducing its observed amplitude. These effects combine to reduce the signal-to-noise by a factor of 2. However, on subhorizon scales, where full second-order codes such as SONG are crucial, the added variance does not limit the detectability.

Here we have included the effects of reionization and the lensing of the bispectrum only in an approximate way, focusing on their impact in the squeezed limit. Reionization could lead to additional intrinsic contributions in a full second-order treatment, while lensing could affect the signal on subhorizon scales. We will examine these questions in future work.

ACKNOWLEDGMENTS

G. W. P. and A. L. acknowledge support by the United Kingdom STFC Grant No. ST/I000976/1; C. F., R. C., K. K. and D. W. are supported by STFC Grants No. ST/K00090/1 and No. ST/L005573/1. The research leading to these results has received funding from the European Research Council under the European Union's Seventh Framework Program (FP/2007-2013)/ERC Grant Agreement No. [616170].

[1] E. Komatsu and D. N. Spergel, Phys. Rev. D **63**, 063002 (2001).
[2] E. Komatsu, Classical Quantum Gravity **27**, 124010 (2010).
[3] M. Liguori, E. Sefusatti, J. R. Fergusson, and E. P. S. Shellard, Adv. Astron. **2010**, 980523 (2010).
[4] A. P. S. Yadav and B. D. Wandelt, Adv. Astron. **2010**, 565248 (2010).
[5] N. Bartolo, S. Matarrese, and A. Riotto, Adv. Astron. **2010**, 157079 (2010).
[6] Planck Collaboration, Astron. Astrophys. **571**, A24 (2014).
[7] A. Gangui, F. Lucchin, S. Matarrese, and S. Mollerach, Astrophys. J. **430**, 447 (1994).
[8] L. Verde, L. Wang, A. F. Heavens, and M. Kamionkowski, Mon. Not. R. Astron. Soc. **313**, 141 (2000).
[9] D. Babich, P. Creminelli, and M. Zaldarriaga, J. Cosmol. Astropart. Phys. 08 (2004) 009.
[10] E. Komatsu, D. N. Spergel, and B. D. Wandelt, Astrophys. J. **634**, 14 (2005).
[11] A. P. S. Yadav, E. Komatsu, and B. D. Wandelt, Astrophys. J. **664**, 680 (2007).
[12] A. P. S. Yadav, E. Komatsu, B. D. Wandelt, M. Liguori, F. K. Hansen, and S. Matarrese, Astrophys. J. **678**, 578 (2008).
[13] D. H. Lyth and Y. Rodríguez, Phys. Rev. Lett. **95**, 121302 (2005).
[14] C. Pitrou, Classical Quantum Gravity **26**, 065006 (2009).
[15] C. Pitrou, J. Uzan, and F. Bernardeau, J. Cosmol. Astropart. Phys. 07 (2010) 003.
[16] M. Beneke and C. Fidler, Phys. Rev. D **82**, 063509 (2010).
[17] A. Naruko, C. Pitrou, K. Koyama, and M. Sasaki, Classical Quantum Gravity **30**, 165008 (2013).
[18] N. Bartolo, S. Matarrese, and A. Riotto, J. Cosmol. Astropart. Phys. 06 (2006) 024.
[19] N. Bartolo, S. Matarrese, and A. Riotto, J. Cosmol. Astropart. Phys. 01 (2007) 019.
[20] N. Bartolo, S. Matarrese, and A. Riotto, J. Cosmol. Astropart. Phys. 01 (2004) 003.
[21] N. Bartolo, S. Matarrese, and A. Riotto, Phys. Rev. Lett. **93**, 231301 (2004).
[22] L. Boubekeur, P. Creminelli, G. D'Amico, J. Noreña, and F. Vernizzi, J. Cosmol. Astropart. Phys. 08 (2009) 029.
[23] L. Senatore, S. Tassev, and M. Zaldarriaga, J. Cosmol. Astropart. Phys. 09 (2009) 038.
[24] L. Senatore, S. Tassev, and M. Zaldarriaga, J. Cosmol. Astropart. Phys. 08 (2009) 031.
[25] D. Nitta, E. Komatsu, N. Bartolo, S. Matarrese, and A. Riotto, J. Cosmol. Astropart. Phys. 05 (2009) 014.
[26] P. Creminelli and M. Zaldarriaga, Phys. Rev. D **70**, 083532 (2004).
[27] P. Creminelli, C. Pitrou, and F. Vernizzi, J. Cosmol. Astropart. Phys. 11 (2011) 025.
[28] N. Bartolo, S. Matarrese, and A. Riotto, J. Cosmol. Astropart. Phys. 02 (2012) 017.
[29] A. Lewis, J. Cosmol. Astropart. Phys. 06 (2012) 023.
[30] Z. Huang and F. Vernizzi, Phys. Rev. Lett. **110**, 101303 (2013).
[31] S.-C. Su, E. A. Lim, and E. P. S. Shellard, Phys. Rev. D **90**, 023004 (2014).
[32] G. W. Pettinari, C. Fidler, R. Crittenden, K. Koyama, and D. Wands, J. Cosmol. Astropart. Phys. 04 (2013) 003.
[33] Z. Huang and F. Vernizzi, Phys. Rev. D **89**, 021302 (2014).
[34] CORE Collaboration, arXiv:1102.2181.

[35] PRISM Collaboration, J. Cosmol. Astropart. Phys. 02 (2014) 006.
[36] C. Fidler, G. W. Pettinari, M. Beneke, R. Crittenden, K. Koyama, and D. Wands, J. Cosmol. Astropart. Phys. 07 (2014) 011.
[37] G. W. Pettinari, arXiv:1405.2280.
[38] U. Seljak and M. Zaldarriaga, Astrophys. J. **469**, 437 (1996).
[39] M. Beneke, C. Fidler, and K. Klingmüller, J. Cosmol. Astropart. Phys. 04 (2011) 008.
[40] S.-C. Su and E. A. Lim, Phys. Rev. D **89**, 123006 (2014).
[41] A. Lewis, A. Challinor, and D. Hanson, J. Cosmol. Astropart. Phys. 03 (2011) 018.
[42] C. Pitrou and A. Stebbins, Gen. Relativ. Gravit. **46**, 1806 (2014).
[43] C. Pitrou, F. Bernardeau, and J.-P. Uzan, J. Cosmol. Astropart. Phys. 07 (2010) 019.
[44] Planck Collaboration, arXiv:1303.5076 [Astron. Astrophys. (to be published)].
[45] L. Pogosian, P. S. Corasaniti, C. Stephan-Otto, R. Crittenden, and R. Nichol, Phys. Rev. D **72**, 103519 (2005).
[46] L. Knox, Phys. Rev. D **52**, 4307 (1995).
[47] D. Hanson, K. M. Smith, A. Challinor, and M. Liguori, Phys. Rev. D **80**, 083004 (2009).
[48] D. N. Spergel and D. M. Goldberg, Phys. Rev. D **59**, 103001 (1999).
[49] D. M. Goldberg and D. N. Spergel, Phys. Rev. D **59**, 103002 (1999).
[50] U. Seljak and M. Zaldarriaga, Phys. Rev. D **60**, 043504 (1999).
[51] A. Cooray, D. Sarkar, and P. Serra, Phys. Rev. D **77**, 123006 (2008).
[52] R. Pearson, A. Lewis, and D. Regan, J. Cosmol. Astropart. Phys. 03 (2012) 011.
[53] M. Zaldarriaga and U. Seljak, Phys. Rev. D **58**, 023003 (1998).
[54] A. Lewis and A. Challinor, Phys. Rep. **429**, 1 (2006).